Proceedings of the 16th European VLBI Network Symposium
Ros, E., Benke, P., Dzib, S., Rottmann, I., & Zensus, J.A. (eds.)
September 2nd-6th 2024, Bonn, Germany

The faint radio nucleus of the megamaser galaxy IC485: AGN or SF activity?

P. Castangia[1], E. Ladu[1,2], A. Tarchi[1], G. Surcis[1], D. Williams-Baldwin[3], F. Panessa[4], J. Braatz[5], and D. Pesce[6]

[1] INAF – Osservatorio Astronomico di Cagliari, Via della Scienza 5, I-09047 Selargius (CA), Italy
[2] Dipartimento di Fisica, Universitá degli Studi di Cagliari, S.P. Monserrato-Sestu km 0,700, I-09042 Monserrato (CA), Italy
[3] Jodrell Bank Centre for Astrophysics, School of Physics and Astronomy, The University of Manchester, Manchester M13 9PL, UK
[4] INAF – Istituto di Astrofisica e Planetologia Spaziali, Via Fosso del Cavaliere 100, I-00133 Roma, Italy
[5] National Radio Astronomy Observatory, 520 Edgemont Road, Charlottesville, VA 22903, USA
[6] Center for Astrophysics – Harvard & Smithsonian, 60 Garden Street, Cambridge, MA 02138, USA

Abstract. Water masers associated with AGNs (the 'megamasers') constitute a unique way to directly map the molecular gas at (sub-)parsec distance from SMBHs and, hence, to study the physical properties, the structure, and the kinematics of the gas surrounding the central engine. In particular, high angular resolution radio continuum and maser observations have been used to test the alignment of the radio jets and the rotation axis of accretion disks and to pinpoint regions of strong interaction of low power jets and/or nuclear outflows with the interstellar medium of the host galaxy in radio quiet AGNs. Presently, we are thoroughly investigating the radio continuum emission in the nucleus of the LINER galaxy IC 485, which hosts a bright H_2O megamaser that, according to our recent 22 GHz VLBI observations might be produced (at least in part) in an edge-on accretion disk. Our recent observations with the e-MERLIN at 1.5 and 5 GHz revealed a flat-spectrum nuclear source, coincident in position with the maser location and with a tentative source visible in our EVN L-band map. The e-MERLIN source is slightly resolved with an orientation of the extended emission approximately perpendicular to that of the putative accretion disk. These characteristics suggest the presence of a weak jet or an outflow in the nucleus of IC 485.

1. Introduction

Luminous (L_{H_2O}>10 $L_\odot$) extragalactic H_2O masers (the 'megamasers') are usually associated with AGN. Very long baseline interferometry (VLBI) observations of this type of masers are the only tool we have to map the molecular gas at (sub-)parsec distance from SMBH and, hence, to study the physical properties, the structure, and the kinematics of the gas surrounding the central engine. These are key ingredients to build detailed models of AGN and investigate AGN feedback processes. Water megamasers may form directly in the nuclear accretion disk, where they can be used to trace the disk geometry and to estimate the rotation velocity and the enclosed nuclear mass (e. g., Kuo et al. 2011; Gao et al. 2017; Zhao et al. 2018). In addition, H_2O masers may also trace nuclear outflows in the form of jets or winds. Jet-maser observations can provide estimates of the shock speeds and densities of radio jets, improving our understanding of the jet-ISM interaction (Gallimore et al. 2001; Peck et al. 2003; Castangia et al. 2019). Water maser observations in Circinus (Greenhill et al. 2003) and NGC 3079 (Kondratko et al. 2005), instead, seem to have resolved individual outflowing torus clouds at <1 pc from the nuclear engine. Proper motion measurements and comparison of these outflow-masers with their disk counterpart offer a promising means to probe the structure and motion of outflowing torus clouds (e. g., Nenkova et al. 2008; Bannikova et al. 2021).

To date, more than 3000 galaxies have been searched for water maser emission and detections have been obtained in about 180 of them[1]. With few exceptions, most of the known maser hosts are radio-quiet AGN classified as Seyfert 2 (Sy 2) or Low-ionization nuclear emission-line regions (LINERs), in the local Universe ($z < 0.05$). Hence, water megamasers also offer a powerful way to shed light on the origin of the radio continuum emission in radio-quiet AGN. Indeed, the origin of the nuclear radio continuum emission in this class of AGN, differently from their radio loud counterpart, may be due to multiple physical mechanisms: in addition to synchrotron emission from relativistic (or sub-relativistic) particles in low-power jets, it might be produced by accretion disk winds and/or coronae, as well as by nuclear star formation (for a review see Panessa et al. 2019). The study of the radio emission in radio quiet AGN, although they constitute the great majority of the AGN population, is, however, challenging due to their intrinsic weakness. High angular resolution radio continuum and H_2O maser observations have been used to test the alignment of the radio jets and the rotation axis

[1] These values are taken from the Megamaser Cosmology Project (MCP) webpage; see also Braatz et al. 2018.

of accretion disks (Kamali et al. 2019) and to pinpoint regions of strong interaction of low power jets and/or nuclear outflows with the interstellar medium of the host galaxies (Peck at al. 2003; Castangia et al. 2019), thus contributing to our understanding of the radio emission mechanism at work in radio quiet AGN

We are currently studying in detail the radio continuum emission in the nucleus of the megamaser galaxy IC 485, where EVN observations at 1.7 and 5 GHz only tentatively detected a radio continuum source (Ladu et al. 2024). With the aim of better constraining the radio continuum emission in IC 485 we recently observed the nuclear region with the e-MERLIN at L- and C-band. Here we present the preliminary results of these new observations.

2. IC 485

Located at a distance of 122 Mpc (the linear scale is $\sim$600 pc/$''$), IC 485 is a spiral galaxy spectroscopically classified as a LINER (Liu et al. 2011), although alternative classifications have been reported in the literature (e.g. Seyfert 2; Kamali et al. 2017). An H_2O megamaser of 900 $L_\odot$ was detected in this galaxy showing a triple-peak profile (Pesce et al. 2015). The sensitive single-dish spectrum together with the accurate position of the maser spots determined through 22 GHz VLBI observations indicate that the maser emission might be produced (at least in part) in an edge-on accretion disk oriented north-south, with a radius of $\sim$0.24 pc (Ladu et al. 2024). K-band HSA observations have been recently obtained together with single-dish line monitoring programs at the GBT and at the SRT, to draw a definite conclusion on the maser nature, and data reduction is in progress (Ladu et al. in prep.).

Unresolved and faint radio continuum emission was detected at kpc-scales with the VLA at 1.4 GHz, with the NVSS ($S_{\rm peak}$=4.4 mJy; Condon 2002) and FIRST ($S_{\rm peak}$=3.01 mJy) surveys. Darling 2017 detected a compact unresolved radio source in the nucleus of IC485 also at 20 GHz, with the VLA, although with a low significance ($S_{\rm peak} = 77 \pm 15\,\mu$Jy, $\sim 5\,\sigma$). Surprisingly, no continuum source was detected above the 5σ noise levels in our EVN maps, neither at 1.4 nor at 5.0 GHz, in a region of 100 mas ($\sim$600 pc) radius from the maser position (Ladu et al. 2024). Nevertheless, a tentative source is visible in the L band map with a peak flux density of 68μJy (3.8 σ). This source coincides in position with the VLA source detected at 20 GHz by Darling (2017) and with the main maser line. The non detection with the EVN suggests that the kpc-scale radio emission observed with the VLA, at lower angular resolution, is mostly resolved out, indicating a diffuse morphology.

3. e-MERLIN observations and data reduction

IC 485 was observed with the e-MERLIN in various observational runs (between March and July 2023 at L-band and in March/April 2023 at C-band, see also Table 1) under project CY15213. The observing set-up for both bands used a total bandwidth of 512 MHz split into eight spectral windows (spw). Each spw had 512 channels but these were averaged to 128 channels as part of the data processing. Scans of the target source were interspersed with scans of the phase calibrator J0802+2509 (target and calibrator scans were 7 min and 3 min long, respectively). We observed the standard e-MERLIN flux density (3C286) and bandpass (OQ208) calibrators at the beginning and/or the end of the observing runs. The data were calibrated using version v1.1.19 of the CASA e-MERLIN pipeline (Moldon 2021). The pipeline flags radio frequency interference (RFI) and performs standard phase and amplitude calibration, bootstraps the flux density scale, calibrates the band pass, and produces diagnostic plots and preliminary images of the calibrators and the target. At the end of the pipeline processing, about 70% and 60% of the scans were flagged, at L- and C-band, respectively, reducing the effective on-source times (Table 1). The array had very few antennas available during the observing runs and this significantly increased the amount of data flagged by the pipeline. We inspected the calibrated data with CASA task PLOTMS to look for any remaining bad visibilities or RFI, especially at the shortest baselines. Outliers were flagged. We then imaged the data with CASA task TCLEAN, using Briggs weighting with a robustness parameter of 0.5. In addition to the full resolution image, we also produced a tapered C-band image, with a *uvtaper* parameter equal to the L-band beam. The full resolution L-band and the tapered C-band maps are shown in Fig. 1, while map details are reported in Table 1.

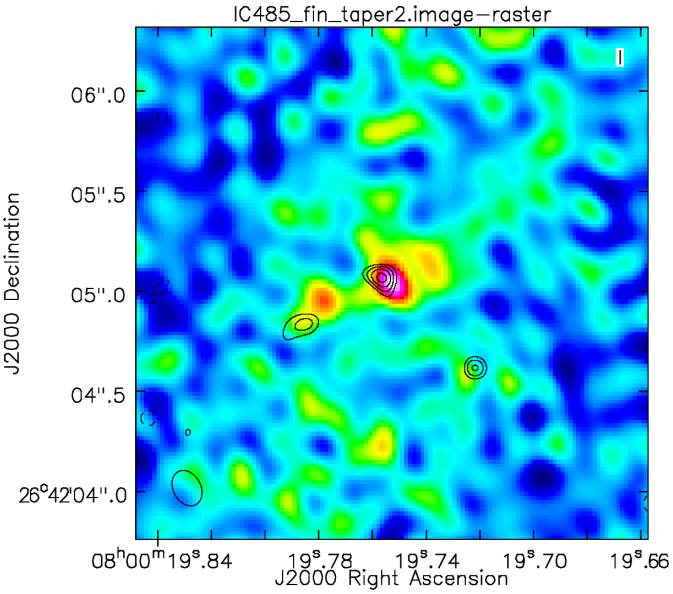

Fig. 1. L-band colour map, with overlaid C-band contours (contour levels are -3, 3, 3.5, 4, 4.5, 5 x 24 μJy/beam). The C-band beam is represented in the lower left corner.

Table 1. e-MERLIN observation and map details.

Band	Obs. date	Frequency (GHz)	$T_{\rm ON}$ (hrs)	% Flagged	$T_{\rm GOOD}$ (hrs)	Synth. beam ($'' \times ''$)	P.A. (°)	*rms* (μJy beam^{-1})
L	28 Mar−13 Jul 2023	1.5	75.60	72%	21.1	0.18×0.12	26	14
C	29 Mar−2 Apr 2023	5.1	12.25	61%	4.8	0.06×0.04	29	14
						0.19×0.15[a]	-11	24

[a] Tapered map.

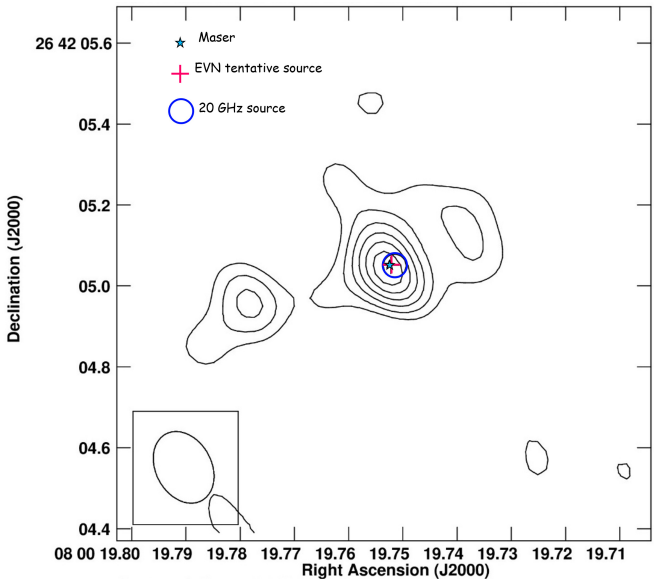

Fig. 2. L-band contours (contour levels are -3, 3, 4, 5, 6, 7, 8, 9, 10 x 14 μJy/beam) with indication of the positions of the maser, the tentative EVN source, and the 20 GHz source detected by Darling (2017).

4. Results and Discussion

Radio continuum emission has been detected toward the nucleus of IC 485 at both frequencies (Fig. 1). The L-band map shows a compact nuclear source surrounded by extended emission approximately in the east-west direction, roughly perpendicular to the putative accretion disk. The compact source is detected also in the tapered C-band map at the 5 σ level (rms=24 μJy/beam). Although with a lower significance, in the C-band image a weak knot is also visible to the east. The peak of the compact source coincides with the maser position, with the tentative source visible in the EVN L-band map, and with the source detected by Darling (2017) with the VLA at K-band (Fig. 2). Peak flux densities are ∼110 microJy at both L- and C-band, indicating that the spectrum is quite flat. Using our e-MERLIN measurements and the 20 GHz flux density reported in Darling (2017) we determined spectral indices between 1.5 GHz and 5 GHz and between 5 GHz and 20 GHz of $\alpha^{5}_{1.5} = 0.04$ and $\alpha^{20}_{5} = -0.17$ ($S \propto \nu^{\alpha}$).

The morphology of the radio emission at e-MERLIN scales (∼100 pc, Fig. 1) is indicative of a small scale jet, as those seen in the L band data of LeMMINGs sample of similar nearby LLAGN (e. g. Baldi et al. 2021). However, the luminosity of the sources ($L_{1.5\rm GHz} = 3.2\times10^{20}$ W Hz^{-1} and $L_{1.5\rm GHz} = 1.1 \times 10^{20}$ W Hz^{-1}, for the central source and the east knot, respectively) and the significance of the extended emission are too low to conclusively state that they are produced by an AGN. The coincidence of the compact central source with the maser and EVN source, together with the flat spectral index are consistent with the basis of a jet or emission from the corona. Nevertheless, the low luminosity of the source does not allow us to completely rule out a star formation origin. A flat spectral index, in fact, is also consistent with free-free thermal emission from HII regions. More sensitive, multi-frequency VLBI observations would be necessary to confidently detect the central source at parsec scale and determine its nature. This would allow us to confirm or reject the presence of a jet in IC 485, shedding light on the origin of the radio continuum emission in this extremely radio quiet AGN.

Acknowledgements. e-MERLIN is a National Facility operated by the University of Manchester at Jodrell Bank Observatory on behalf of STFC, part of UK Research and Innovation.

References

Baldi, R. D., Williams, D. R. A., McHardy, I. M., et al. 2021, MNRAS, 500, 4749
Bannikova, E. Yu., Sergeyev, A. V., Akerman, N. A., et al. 2021, MNRAS, 503, 1459
Braatz, J., Reid, M. J., Humphreys, E. M. L., et al. 2018, in Astrophysical Masers: Unlocking the Mysteries of the Universe, eds. A. Tarchi, M. J. Reid, P. Castangia, IAU Symp., 336, 86
Castangia, P., Tarchi, A., Henkel, C., et al. 2019, A&A, 629, A25
Condon, J. J., Cotton, W. D., & Broderick, J. J. 2002, AJ, 124, 675
Darling, J. 2017, ApJ, 837, 100
Gallimore, J. F., Henkel, C., Baum, S. A., et al. 2001, ApJ, 556, 694
Gao, F., Braatz, J. A., Reid, M. J., et al. 2017, ApJ, 834, 52
Greenhill, L. J., Booth, R. S., Ellingsen, S. P., et al. 2003, ApJ, 590, 162
Kamali, F., Khosroshahi, H. G., Gozaliasl, G., et al. 2017, A&A, 605, A84
Kamali, F., Gozaliasl, G., Khosroshahi, H. G., et al. 2019, A&A, 624, A42
Kondratko, P. T., Greenhill, L. J., & Moran, J. M. 2005, ApJ, 618, 618
Kuo, C. Y., Braatz, J. A., Condon, J. J., et al. 2011, ApJ, 727, 20
Ladu, E., Tarchi, A., Castangia, P., et al. 2024, A&A, 682, A25

Liu, X., Shen, Y., Strauss, M. A., & Greene, J. E. 2011, ApJ, 737, 101
Moldon, J. 2021, eMCP: e-MERLIN CASA pipeline, Astrophysics Source Code Library, ascl:2109.006
Nenkova, M., Sirocky, M. M., Nikutta, R., et al. 2008, ApJ, 685, 160
Panessa, F., Baldi, R. D., Laor, A., et al. 2019, NatAs, 3, 387
Peck, A. B., Henkel, C., Ulvestad, J. S., et al. 2003, ApJ, 590, 149
Pesce, D. W., Braatz, J. A., Condon, J. J., et al. 2015, ApJ, 810, 65
Zhao, W., Braatz, J. A., Condon, J. J., et al. 2018, ApJ, 854, 124